ACS OMEGA

Article

Cite This: ACS Omega XXXX, XXX, XXX−XXX

http://pubs.acs.org/journal/acsodf

Azide-Based High-Energy Metal−Organic Frameworks with Enhanced Thermal Stability

Ignacio Chi-Durán,[†,‡] Javier Enríquez,[†,§] Carolina Manquián,[†,§] Rubén Alejandro Fritz,[†,‡] Andrés Vega,[∥] Daniel Serafini,[†] Felipe Herrera,*[,†,‡] and Dinesh Pratap Singh*[,†,‡]

[†]Department of Physics, University of Santiago Chile, Avenida Ecuador 3493, Estación Central, 9170124 Santiago, Chile

[‡]Millennium Institute for Research in Optics (MIRO), Av. Esteban Iturra S/N, Concepción, 4030000 Concepción, Chile

[§]Department of Metallurgical Engineering, Faculty of Engineering, University of Santiago Chile, Av. Lib. Bernardo O' Higgins 3363, Estación Central, 9170022 Santiago, Chile

[∥]Departamento de Ciencias Químicas, Facultad de Ciencias Exactas, Universidad Andrés Bello, Av. República 498, 8370251 Santiago, Chile

Supporting Information

ABSTRACT: We describe the structure and properties of $[Zn(C_6H_4N_5)N_3]_n$, a new nonporous three-dimensional high-energy metal−organic framework (HE-MOF) with enhanced thermal stability. The compound is synthesized by the hydrothermal method with in situ ligand formation under controlled pH and characterized using single-crystal X-ray diffraction, elemental analysis, and Fourier transform infrared. The measured detonation temperature (T_{det} = 345 °C) and heat of detonation (ΔH_{det} = −0.380 kcal/g) compare well with commercial explosives and other nitrogen-rich HE-MOFs. The velocity and pressure of denotation are 5.96 km/s and 9.56 GPa, respectively. Differential scanning calorimetry analysis shows that the denotation of $[Zn(C_6H_4N_5)N_3]_n$ occurs via a complex temperature-dependent mechanism.

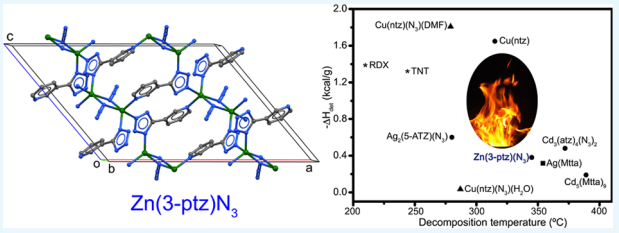

INTRODUCTION

Metal−organic frameworks (MOFs) have attracted great interest in materials science due to the large combination of organic ligands and inorganic building blocks that can be used to produce novel crystalline structures with desired properties. This structural diversity has enabled applications in gas storage,[1−3] gas separation,[4−6] nonlinear optics,[7−9] drug delivery,[10−12] catalysis,[13,14] and sensing.[15,16] Recently, high-energy metal−organic frameworks (HE-MOFs) have emerged as promising energetic materials due to their facile synthesis, higher density, better thermal stability, and superior mechanical strength in comparison with conventional energetic compounds.[17−22]

HE-MOFs should ideally have high density, elevated heat of detonation, insensitivity to mechanical stress, and high thermal stability.[23−29] High heats of detonation can be reached using nitrogen-rich compounds, which have large average bond energies, such as C−N (273 kJ mol^{-1}), N−N (160 kJ mol^{-1}), N═N (418 kJ mol^{-1}), and N≡N (954 kJ mol^{-1}).[17] One promising strategy to design HE-MOFs involves the use of five-membered nitrogen heterocycles as ligands. In particular, pyrazole and tetrazole molecules are promising choices due to their high heats of formation, elevated nitrogen content, stability, and multiple coordination sites with commonly used transition metal ions.[30−35] Azido ligands can also be used to assemble HE-MOFs by introducing the N≡N bond into the crystal structure, although the azido group often decreases the thermal stability of materials, decreasing their energetic performance. To increase the thermal stability of HE-MOFs, three-dimensional (3D) coordination geometries result in superior structural reinforcement of the energetic groups.[36]

In this work, we describe the energetic properties of $[Zn(C_6H_4N_5)N_3]_n$ (1), a new 3D HE-MOF that stabilizes 3-pyridyltetrazole and azido ligands in its structure. The obtained structure compares well in terms of energetic group density, detonation enthalpy, and detonation temperature with respect to other MOF structures that have similar functional groups, as well as commercial explosives (see Figure 1). Our synthesis strategy involves the in situ formation of 3-pyridyltetrazole ligands in the presence of azide and cyano-compounds, via a Demko-Sharpless reaction involving Zn^{2+} as a Lewis acid.[37] This strategy avoids sequential synthesis steps and the use of environmentally toxic solvents or commonly used heavy metal ions such as Pb^{2+} and Ag^{+}.

RESULTS AND DISCUSSION

Structural Analysis. Fourier transform infrared (FTIR) analysis shows an intense sharp peak for asymmetric stretching

Received: April 18, 2019
Accepted: August 9, 2019

DOI: 10.1021/acsomega.9b01127
ACS Omega XXXX, XXX, XXX−XXX

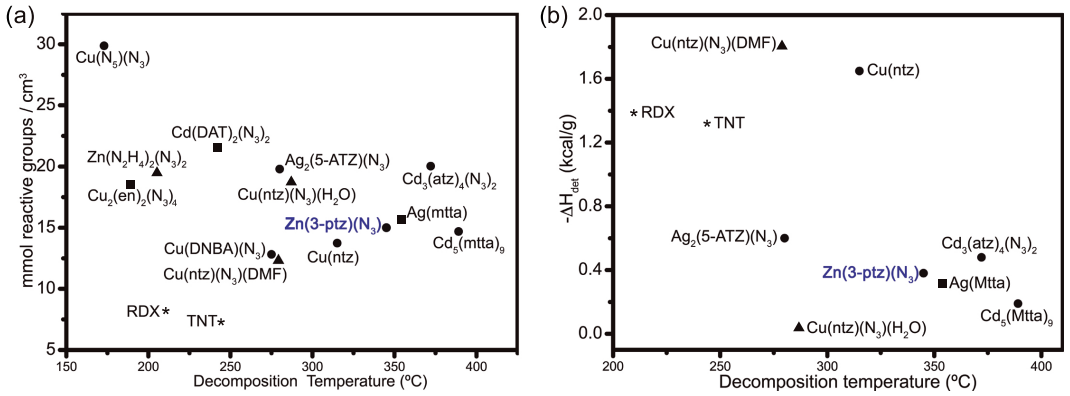

Figure 1. Energetic properties for selected high-energy MOFs with azole and azide-based ligands. (a) Map of volume density of energetic groups (azole, azido) in the crystal lattice and decomposition temperature. (b) Map of heat of denotation (ΔH_{det}) and their decomposition temperature. Commercial explosives RDX and TNT are shown for comparison (*). (ntz): 3-nitro-1,2,4-triazolate; (DAT): 1,5-diaminotetrazolate; (en): ethylenediamine; (atz): 3-amino-1,2,4-triazolate; (DNBA): 3,5-dinitrobenzoic acid. The maps include 1D (▲), 2D (■), and 3D (●) coordination geometries.

at 2075 cm^{-1} and a second band for the symmetric stretching of the azido group at 1281 cm^{-1} (Figure 2). In addition, the

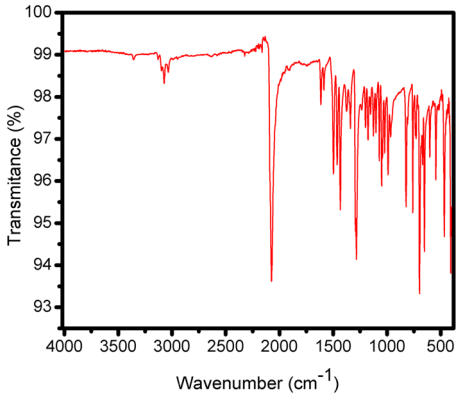

Figure 2. FTIR spectra of $Zn(3\text{-ptz})N_3$.

tetrazole ring of compound (**1**) shows peaks in the region 1640−1335 cm^{-1} as reported for similar structures.[32,33] The aromatic C−H stretching and out-of-plane bands at 3069 and 700 cm^{-1}, respectively, are both assigned to the pyridine ring. Single-crystal X-ray diffraction (XRD) shows that compound (**1**) belongs to the monoclinic crystal system and *C*2/*c* space group (see Table 1). The asymmetric unit is composed of a Zn atom, coordinated to both azide and 3-pyridyltetrazole molecules (Figure 3a). The zinc(II) cation presents a distorted trigonal bipyramidal orbital geometry, in which the nitrogens N1, N5, and N6 from tetrazolide, pyridyl, and azido ligands, respectively, are displaced in the equatorial plane, involving a bond length ranging between 1.9837(16) and 2.0632(15) Å (see Table S2). Axial nitrogens N3 and N6 from azido and tetrazolide groups form coordination bonds with lengths in the range 2.1826(15)−2.3585(16) Å. Figure 3b shows the presence of azido groups in the axial and equatorial positions leading to a symmetrical arrangement of two trigonal bipyrimidal units related by point symmetry and bonded through azido bridges by a μ-1,1 coordination mode. Compound (**1**) shows a three-dimensional coordination framework, in which the azido groups are oriented into the cavities when observed along the 010 direction (see Figure S1). Molecular dynamics modeling shows that (**1**) has a

Table 1. Crystallographic Data for $Zn(3\text{-ptz})N_3$

CCDC number	1857180
empirical formula	$Zn(C_6H_4N_5)N_3$
formula weight/g mol^{-1}	253.52
crystal system	monoclinic
space group	*C*2/*c* (N °15)
T/K	296
a/Å	20.519(4)
b/Å	7.6959(15)
c/Å	14.708(5)
β/deg	130.239(2)
Z	8
ρ_c/g cm^{-3}	1.900
$R(F)^a$	0.0219
$R_w(F^2)^b$	0.0563

$^aR(F) = \sum||F_o| - |F_c||/\sum|F_o|$. $^bR_w(F^2) = [\sum_w(F_o^2 - F_c^2)^2/\sum_w(F_o^2)^2]^{1/2}$.

helium void fraction of 0.027 and is thus nonporous. This prediction was confirmed in N_2 gas adsorption experiments (ESI).

Thermal Decomposition. Good thermal stability is a desired feature in energetic materials because low decomposition temperatures limit their performance in applications. To assess the thermal stability of (**1**), we performed thermogravitmetric (TG) and differential scanning calorimetry (DSC) analyses. The results are shown in Figure 4. The TG curve shows that there is negligible mass loss up to 325 °C, where about 49% of the initial weight is lost in an intense mass-loss process that occurs over a small temperature range. The DSC data show a very intense exothermic peak at 345 °C. In comparison with similar azide-based MOFs such as $Cu(DNBA)N_3$[38] and $Ag_2(5\text{-ATZ})N_3$,[39] the detonation temperature of compound (**1**) is much higher. In $Ag_2(5\text{-ATZ})N_3$, silver atoms coordinate with 5-amino-tetrazole and azide ligands in a similar way to that in (**1**). The enhanced thermostability observed in (**1**) is possibly due to the bipyramidal coordination environment, in contrast to the tetrahedral coordination geometry found in $Ag_2(5\text{-ATZ})N_3$. For comparison, we list in Table 2 the energetic properties of (**1**) and other energetic materials.

Energy of Combustion and Enthalpy of Formation. The constant-volume energy of combustion of (**1**) was measured using an oxygen-bomb calorimeter. From ΔH =

DOI: 10.1021/acsomega.9b01127
ACS Omega XXXX, XXX, XXX−XXX

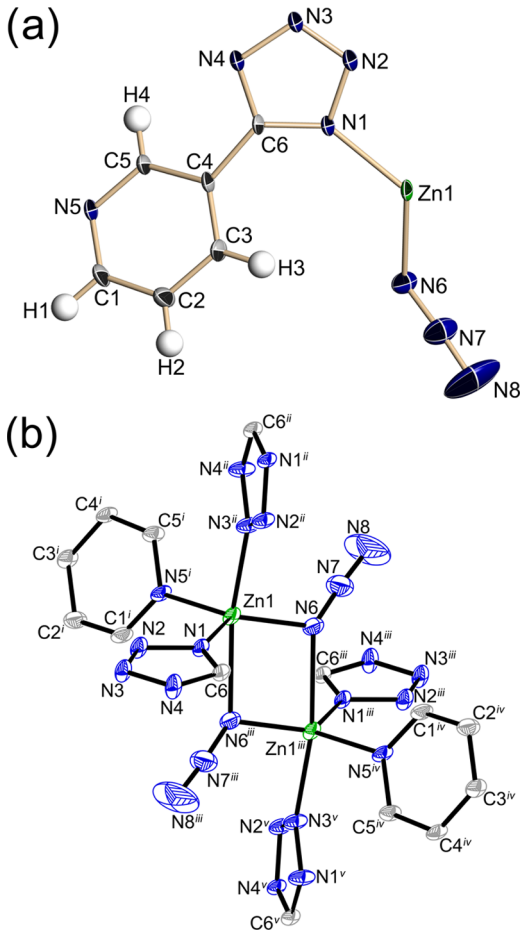

Figure 3. (a) Thermal ellipsoid plot of the asymmetric unit of compound (**1**) with the 50% probability level, whereas hydrogen atoms are drawn as spheres of arbitrary radii. (b) Thermal ellipsoid plot of symmetrical molecular arrangement. Hydrogens are omitted for clarity. Symmetry codes: (i) $-1/2 + x, 3/2 - y, -1/2 + z$; (ii) $1/2 - x, 1/2 + y, 1/2 - z$; (iii) $1/2 - x, 3/2 - y, - z$; (iv) $1 - x, y, 1/2 - z$; and (v) $x, 1 - y, -1/2 + z$.

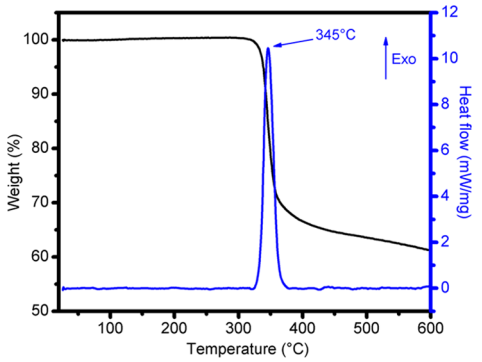

Figure 4. Thermogravimetric and DSC curves of compound (**1**).

$Q_p = Q_v + \Delta nRT$, with a bomb combustion equation of the form

$$ZnC_6H_4N_{8(s)} + 7.5O_{2(g)} \rightarrow ZnO_{(s)} + 6CO_{2(g)} + 2H_2O_{(l)} + 4N_{2(g)} \quad (1)$$

we obtain the enthalpy of combustion $\Delta_c H = -3623$ kJ mol^{-1}, which is higher than commercial explosives such as TNT (-3406 kJ mol^{-1}),[40] RDX (-2120 kJ mol^{-1}), and HMX (-2820 kJ mol^{-1}).[41] This high enthalpy can be understood from the oxidation involved in the aromatic ring breaking. From the Hess law, we obtain the enthalpy of formation $\Delta_f H^\circ_{298}$(**1**,s) = 339 kJ mol^{-1}.[42]

Detonation Parameters. The energy of detonation is one of the most important parameters that determine the performance of an energetic material. Following the method proposed in refs 43, 44, the detonation reaction for compound (**1**) can be written as

$$ZnC_6H_4N_{8(s)} \rightarrow Zn_{(s)} + 6C_{(s)} + \frac{4}{3}NH_{3(g)} + \frac{10}{3}N_{2(g)} \quad (2)$$

We estimate the energy of detonation from the enthalpies of formation using the relation

$$\Delta H_{det} = \frac{\sum \Delta H_f(\text{products}) - \Delta H_f(\text{MOF})}{MW} \quad (3)$$

where MW is the molecular weight of $ZnC_6H_4N_8$. The estimated enthalpy of detonation is -0.38 kcal g^{-1}.

Structural analysis based on the volume density of reactive groups as a function of their thermal stability (Figure 1a) shows that structures with highly reactive group density tend to have poor thermal stability. The three-dimensional structure of (**1**) and its moderate energetic group density therefore explain the enhanced thermal stability observed. Figure 1b shows that structures with azoles substituted with nitro groups (ntz) and organic nitro compounds (TNT and RDX) tend to have higher ΔH_{det} than nonoxygen containing groups such as 3-ptz but have much lower thermal stabilities.

The detonation velocity (D) and detonation pressure (P) of (**1**) can be obtained from ΔH_{det} and the semiempirical equations in ref 43 using the expressions

$$D = 1.01(NM^{1/2}Q^{1/2})^{1/2}(1 + 1.30\rho) \quad (4)$$

and

$$P = 1.558N(MQ)^{1/2}\rho^2 \quad (5)$$

where the detonation velocity is in units of km/s, and the detonation pressure is in GPa. ρ is the density of the energetic material in g/cm^3, N is the number of moles of gaseous detonation products per gram of energetic material, M is the average of molecular weight of gases, and Q is the detonation heat of the reaction in cal/g. Using the parameters of (**1**), we obtain D = 5.96 km/s and P = 9.56 GPa (see Table 2). These values are consistent with the relatively low energy of formation and low oxygen content of (**1**), which decrease the enthalpy of detonation and the molar mass average of the gas products. Despite the low oxygen content, the obtained heat of detonation of (**1**) is higher than other energetic MOFs with tetrazole ligands as shown (see Figure 1b).

Kinetic Analysis. To study the kinetic behavior of (**1**), we performed DSC measurements at different heating rates β = 1, 5, 10, 15, and 20 °C/min. The DSC peak displaces to higher temperatures as β increases, until reaching a plateau for $\beta \geq 10$ °C/min. At the highest heating rates, additional smaller peaks at temperatures beyond the main decomposition temperature appear. The scaling of the decomposition temperature with β could not be fitted using the Kissinger and Ozawa–Doyle kinetic models,[45−47] which points to a temperature-dependent multistep decomposition mechanism. This behavior is different

DOI: 10.1021/acsomega.9b01127
ACS Omega XXXX, XXX, XXX−XXX

Table 2. Physicochemical Properties of $Zn(3\text{-ptz})N_3$ and Selected Energetic Materials

compound	ρ^a	N^b	Ω^c	$T_{dec}{}^d$	$\Delta_f H^\circ_{298}{}^e$	Q^f	D^g	P^h
$Zn(3\text{-ptz})N_3$	1.900	44.20	−94.86	345	339	0.38	5.96	9.56
$Cd_3(atz)_4(N_3)_2$	2.517	40.89	−40.33	372	1330	0.480	5.92	18.61
Ag(Mtta)	2.995	29.34	−4.68	354	206	0.316	5.26	15.83
RDX	1.806	37.80	−21.60	210	93	1.44	8.91	34.1
TNT	1.654	18.50	−73.96	295	−67	1.22	7.18	20.50

[a]Density calculated by single-crystal X-ray diffraction (g cm^{-3}). [b]Nitrogen content (%). [c]Oxygen balance (%). [d]Decomposition temperature (°C). [e]Enthalpy of formation (kJ mol^{-1}). [f]Heat of detonation (kcal g^{-1}). [g]Detonation velocity (km s^{-1}). [h]Detonation pressure (GPa); Mtta: 5-methyltetrazolate; atz: 3-amino-1,2,4-triazolate.

from commercial explosives such as TNT and RDX, which fit well to the Kissinger model.[48]

CONCLUSIONS

We describe the synthesis and energetic properties of a new three-dimensional high-energy MOF with excellent thermal stability up to 345 °C. The compound has azido and tetrazole ligands in its structure and is obtained via the hydrothermal method with in situ ligand formation. The reported MOF exhibits higher thermostability than typical explosives and other three-dimensional MOFs. The measured enthalpy of combustion ($\Delta_c H$ = −3623 kJ/mol) is higher than TNT, RDX, and HMX, but the measured heat of detonation is moderate, possibly due to the relatively low oxygen content in the structure. The detonation velocity was found to be D = 5.96 km/s and the pressure of detonation P = 9.56 GPa. To better assess the potential advantage in applications of this new high-energy MOF relative to commercial explosives, further characterization of its chemical stability, mechanical stability, and detonation velocities needs to be done. Moreover, differential scanning calorimetry measurements reveal that the decomposition kinetics cannot be explained using Kissinger and Owaza−Doyle models, which suggests a complex decomposition mechanism that has yet to be understood.

EXPERIMENTAL SECTION

Caution. Although no explosive behavior was observed during the synthesis, growing and handling of HE-MOFs or azido complexes are known to be potentially explosive. Small-scale synthesis is strongly encouraged. Manipulations must be carried out in a hood behind a safety shield. Eye protection and leather gloves must be worn at all times.

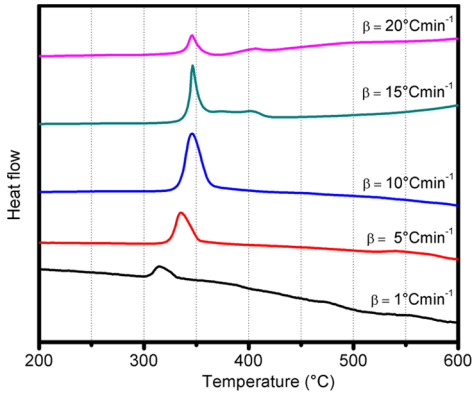

Figure 5. DSC curves for different heating rates β = 1, 5, 10, 15, and 20 °C min^{-1}.

Materials and Methods. The crystal structures of both solvates were determined by X-ray diffraction at 293 K. Data collection was done on a SMART CCD diffractometer using f- and o-scans as the data collection strategy. Data sets were reduced using SAINT,[49] while the structures were solved by direct methods and completed by Difference Fourier Synthesis for nonhydrogen atoms. Least-squares refinement was conducted by using SHELXL.[50] (Multiscan absorption corrections were applied using SADABS.[49]) The hydrogen atom positions were calculated after each cycle of refinement with SHELXL using a riding model for each structure, with a C−H distance of 0.93 Å. $U_{iso}(H)$ values were set equal to 1.2 U_{eq} of the parent carbon atom. The thermogravimetric analyses were done on a Mettler Toledo model TGA/DSC 2 Star equipment. The TGA curves were registered in the 20−600 °C range, using a 10 °C/min heating rate under nitrogen atmosphere (40 mL/min). DSC experiments were performed at 1, 5, 10, 15 and 20 °C/min. IR spectra was recorded on a Spectrum Two FTIR Spectrometer. The elemental analyses were done on a FLASH 2000 CHN Analyzer equipment. Powder X-ray diffraction analysis was done using a Shimadzu XRD 6000 diffractometer with Cu Kα (l = 1.5418 Å) radiation for structural characterization and phase determination. Calculated PXRD patterns were generated using Mercury 3.10. The constant-volume energy of combustion was measured in an oxygen-bomb calorimeter (Parr 6200, Parr instruments Company, Illinois, USA) and using samples of 0.55 g according to UNE-EN 14918 standard for biosolid fuels. Finally, all reactants were used without purification and the pH was monitored using a pH 2700 Oakton pH meter. Textural properties were obtained from the adsorption−desorption isotherm of N_2 at 77 K, which was carried out using a Micromeritics 3Flex instrument. The sample was previously degassed for 10 h at 413 K under vacuum using a Micromeritics Smart VacPrep instrument. All gas-intake simulations were performed assuming a rigid MOF structure using the grand canonical Monte Carlo molecular simulation scheme on the software RASPA.[51] A 2 × 4 × 3 supercell for calculation was set to use a 12 Å cutoff for the intermolecular interactions in the system. Five thousand cycles of initialization and another five thousand for the actual ensemble average simulations were done totalizing 10 000 cycles. Partial atomic charges for the atoms of the framework were obtained by the charge equilibration method (QEq). Generic MOFs and Trappe force-field definitions were employed for the MOF atoms and the N_2 and CO_2 gases, respectively. Temperatures for the isotherm estimation were 77 K in the N_2 case and 274 K for CO_2.

Synthesis of $Zn(3\text{-ptz})N_3$ (1). All of the reactants and chemicals were purchased from Sigma-Aldrich and utilized without further purification. A mixture of 3-cyanopyridine (4

DOI: 10.1021/acsomega.9b01127
ACS Omega XXXX, XXX, XXX−XXX

mmol), NaN_3 (8 mmol), and $Zn(CH_3COO)_2$ (8 mmol) were dissolved in 6 mL of distilled water. The pH value was adjusted by using HNO_3 (66%) until reaching pH in the range 2.7−2.8. The mixture was transferred into a glass bottle and then put in a box furnace at 105 °C for 24 h. The as-synthesized materials were taken out of the furnace after 24 h, filtered, and dried at room temperature prior to the structural analysis. Elem. anal. calcd (%) for $Zn(C_6H_4N_5)N_3$ (253.52): C, 28.49; N, 44.17; H, 1.57. Found: C, 27.89; N, 42.08; H, 1.50.(Figure 5)

■ ASSOCIATED CONTENT

Supporting Information

The Supporting Information is available free of charge on the ACS Publications website at DOI: 10.1021/acsomega.9b01127.

View along the [010] direction of (**1**); adsorption−desorption isotherms of N_2 for (**1**); Kissinger and Ozawa−Doyle model plots for (**1**) (ZIP)

Crystallography tables, adsorption measurements, powder X-ray diffraction, and kinetic plots (PDF)

Data_SCD18_104_C2c (CIF)

■ AUTHOR INFORMATION

Corresponding Authors

*E-mail: felipe.herrera.u@usach.cl (F.H.).

*E-mail: singh.dinesh@usach.cl, dineshpsingh@gmail.com (D.P.S.).

ORCID

Ignacio Chi-Durán: 0000-0002-3327-2825

Javier Enríquez: 0000-0002-2502-5787

Andrés Vega: 0000-0001-6501-4161

Felipe Herrera: 0000-0001-8121-1931

Dinesh Pratap Singh: 0000-0002-2893-7749

Notes

The authors declare no competing financial interest.

■ ACKNOWLEDGMENTS

F.H. was supported by CONICYT through the Proyecto REDES ETAPA INICIAL, Convocatoria 2017 No. REDI 170423, and FONDECYT Regular No. 1181743. D.P.S. and F.H. are grateful for support by Millennium Scientific Initiative (ICM) through the Millennium Institute for Research in Optics (MIRO).

■ REFERENCES

(1) Farha, O. K.; Yazaydın, A. Ö.; Eryazici, I.; Malliakas, C. D.; Hauser, B. G.; Kanatzidis, M. G.; Nguyen, S. T.; Snurr, R. Q.; Hupp, J. T. De novo synthesis of a metal-organic framework material featuring ultrahigh surface area and gas storage capacities. *Nat. Chem.* **2010**, *2*, 944−948.

(2) Furukawa, H.; Ko, N.; Go, Y. B.; Aratani, N.; Choi, S. B.; Choi, E.; Yazaydin, A. Ö.; Snurr, R. Q.; O'Keeffe, M.; Kim, J.; Yaghi, O. M. Ultrahigh porosity in metal-organic frameworks. *Science* **2010**, *329*, 424−428.

(3) Du, L.; Lu, Z.; Zheng, K.; Wang, J.; Zheng, X.; Pan, Y.; You, X.; Bai, J. Fine-tuning pore size by shifting coordination sites of ligands and surface polarization of metal-organic frameworks to sharply enhance the selectivity for CO2. *J. Am. Chem. Soc.* **2013**, *135*, 562−565.

(4) Bloch, E. D.; Queen, W. L.; Krishna, R.; Zadrozny, J. M.; Brown, C. M.; Long, J. R. Hydrocarbon separations in a metal-organic framework with open iron (II) coordination sites. *Science* **2012**, *335*, 1606−1610.

(5) Gu, Z.-Y.; Yan, X.-P. Metal-organic framework MIL-101 for high-resolution gas-chromatographic separation of xylene isomers and ethylbenzene. *Angew. Chem., Int. Ed.* **2010**, *49*, 1477−1480.

(6) Bae, T.-H.; Lee, J. S.; Qiu, W.; Koros, W. J.; Jones, C. W.; Nair, S. A high-performance gas-separation membrane containing submicrometer-sized metal-organic framework crystals. *Angew. Chem.* **2010**, *122*, 10059−10062.

(7) Yu, J.; Cui, Y.; Wu, C.; Yang, Y.; Wang, Z.; O'Keeffe, M.; Chen, B.; Qian, G. Second-order nonlinear optical activity induced by ordered dipolar chromophores confined in the pores of an anionic metal-organic framework. *Angew. Chem.* **2012**, *124*, 10694−10697.

(8) Zou, J.-P.; Peng, Q.; Wen, Z.; Zeng, G.-S.; Xing, Q.-J.; Guo, G.-C. Two Novel Metal- Organic Frameworks (MOFs) with (3, 6)-Connected Net Topologies: Syntheses, Crystal Structures, Third-Order Nonlinear Optical and Luminescent Properties. *Cryst. Growth Des.* **2010**, *10*, 2613−2619.

(9) Wang, C.; Zhang, T.; Lin, W. Rational synthesis of noncentrosymmetric metal-organic frameworks for second-order nonlinear optics. *Chem. Rev.* **2012**, *112*, 1084−1104.

(10) Huxford, R. C.; Della Rocca, J.; Lin, W. Metal-organic frameworks as potential drug carriers. *Curr. Opin. Chem. Biol.* **2010**, *14*, 262−268.

(11) Della Rocca, J.; Liu, D.; Lin, W. Nanoscale metal-organic frameworks for biomedical imaging and drug delivery. *Acc. Chem. Res.* **2011**, *44*, 957−968.

(12) Horcajada, P.; Chalati, T.; Serre, C.; Gillet, B.; Sebrie, C.; Baati, T.; Eubank, J. F.; Heurtaux, D.; Clayette, P.; Kreuz, C.; Chang, J.-S.; Hwang, Y. K.; Marsaud, V.; Bories, P.-N.; Cynober, L.; Gil, S.; Férey, G.; Couvreur, P.; Gref, R. Porous metal-organic-framework nanoscale carriers as a potential platform for drug delivery and imaging. *Nat. Mater.* **2010**, *9*, 172−178.

(13) Liu, J.; Chen, L.; Cui, H.; Zhang, J.; Zhang, L.; Su, C.-Y. Applications of metal-organic frameworks in heterogeneous supramolecular catalysis. *Chem. Soc. Rev.* **2014**, *43*, 6011−6061.

(14) Yoon, M.; Srirambalaji, R.; Kim, K. Homochiral metal-organic frameworks for asymmetric heterogeneous catalysis. *Chem. Rev.* **2012**, *112*, 1196−1231.

(15) Campbell, M. G.; Sheberla, D.; Liu, S. F.; Swager, T. M.; Dincă, M. Cu3 (hexaiminotriphenylene) 2: an electrically conductive 2D metal-organic framework for chemiresistive sensing. *Angew. Chem., Int. Ed.* **2015**, *54*, 4349−4352.

(16) Kreno, L. E.; Leong, K.; Farha, O. K.; Allendorf, M.; Van Duyne, R. P.; Hupp, J. T. Metal-organic framework materials as chemical sensors. *Chem. Rev.* **2012**, *112*, 1105−1125.

(17) Zhang, S.; Yang, Q.; Liu, X.; Qu, X.; Wei, Q.; Xie, G.; Chen, S.; Gao, S. High-energy metal-organic frameworks (HE-MOFs): Synthesis, structure and energetic performance. *Coord. Chem. Rev.* **2016**, *307*, 292−312.

(18) Fedoroff, B.; Sheffield, O. *Encyclopedia of Explosives and Related Items*; Picatinny Arsenal: Dover, NJ, 1966; Vol. *5*, pp C169−C172.

(19) Davis, T. *The Chemistry of Powder and Explosives*; Angriff: Los Angeles, 1943; pp 443−446.

(20) Huynh, M. H. V.; Hiskey, M. A.; Archuleta, J. G.; Roemer, E. L.; Gilardi, R. 6-Di (azido)-1, 2, 4, 5-Tetrazine: A Precursor for the Preparation of Carbon Nanospheres and Nitrogen-Rich Carbon Nitrides. *Angew. Chem., Int. Ed.* **2004**, *43*, 5658−5661.

(21) Chavez, D. E.; Hiskey, M. A.; Naud, D. L. Tetrazine explosives. *Propellants, Explos., Pyrotech.* **2004**, *29*, 209−215.

(22) Keßenich, E.; Klapötke, T. M.; Knizek, J.; Nöth, H.; Schulz, A. Characterization, Crystal Structure of 2, 4-Bis (triphenylphosphanimino) tetrazolo [5, 1-a]-[1, 3, 5] triazine, and Improved Crystal Structure of 2, 4, 6-Triazido-1, 3, 5-triazine. *Eur. J. Inorg. Chem.* **1998**, *1998*, 2013−2016.

(23) Feng, Y.; Bi, Y.; Zhao, W.; Zhang, T. Anionic metal-organic frameworks lead the way to eco-friendly high-energy-density materials. *J. Mater. Chem. A* **2016**, *4*, 7596−7600.

(24) Zhang, Y.; Zhang, S.; Sun, L.; Yang, Q.; Han, J.; Wei, Q.; Xie, G.; Chen, S.; Gao, S. A solvent-free dense energetic metal-organic

DOI: 10.1021/acsomega.9b01127
ACS Omega XXXX, XXX, XXX−XXX

framework (EMOF): to improve stability and energetic performance via in situ microcalorimetry. *Chem. Commun.* **2017**, *53*, 3034−3037.
(25) Seth, S.; McDonald, K. A.; Matzger, A. J. Metal Effects on the Sensitivity of Isostructural Metal-Organic Frameworks Based on 5-Amino-3-nitro-1 H-1, 2, 4-triazole. *Inorg. Chem.* **2017**, *56*, 10151−10154.
(26) Gu, H.; Ma, Q.; Huang, S.; Zhang, Z.; Zhang, Q.; Cheng, G.; Yang, H.; Fan, G. Gem-dinitromethyl-substituted Energetic Metal-Organic Framework based on 1, 2, 3-Triazole from in situ Controllable Synthesis. *Chem. - Asian J.* **2018**, *13*, 2786−2790.
(27) Ma, X.; Liu, Y.; Song, W.; Wang, Z.; Liu, X.; Xie, G.; Chen, S.; Gao, S. A difunctional azido-cobalt (II) coordination polymer exhibiting slow magnetic relaxation behaviour and high-energy characteristics with good thermostability and insensitivity. *Dalton Trans.* **2018**, *47*, 12092−12104.
(28) Li, W.; Wang, K.; Qi, X.; Jin, Y.; Zhang, Q. Construction of a Thermally Stable and Highly Energetic Metal-Organic Framework as Lead-Free Primary Explosives. *Cryst. Growth Des.* **2018**, *18*, 1896−1902.
(29) Shen, C.; Xu, Y.-g.; Lu, M. A series of high-energy coordination polymers with 3, 6-bis (4-nitroamino-1, 2, 5-oxadiazol-3-yl)-1, 4, 2, 5-dioxadiazine, a ligand with multi-coordination sites, high oxygen content and detonation performance: syntheses, structures, and performance. *J. Mater. Chem. A* **2017**, *5*, 18854−18861.
(30) Zhao, H.; Qu, Z.-R.; Ye, H.-Y.; Xiong, R.-G. In situ hydrothermal synthesis of tetrazole coordination polymers with interesting physical properties. *Chem. Soc. Rev.* **2008**, *37*, 84−100.
(31) Wu, B.-D.; Zhou, Z.-N.; Li, F.-G.; Yang, L.; Zhang, T.-L.; Zhang, J.-G. Preparation, crystal structures, thermal decompositions and explosive properties of two new high-nitrogen azide ethylenediamine energetic compounds. *New J. Chem.* **2013**, *37*, 646−653.
(32) Chi-Durán, I.; Enríquez, J.; Manquian, C.; Wrighton-Araneda, K.; Cañon-Mancisidor, W.; Venegas-Yazigi, D.; Herrera, F.; Singh, D. P. pH-Controlled Assembly of 3D and 2D Zinc-Based Metal-Organic Frameworks with Tetrazole Ligands. *ACS Omega* **2018**, *3*, 801−807.
(33) Enríquez, J.; Manquian, C.; Chi-Duran, I.; Herrera, F.; Singh, D. P. Controlled Growth of the Noncentrosymmetric Zn (3-ptz) 2 and Zn (OH)(3-ptz) Metal-Organic Frameworks. *ACS Omega* **2019**, *4*, 7411−7419.
(34) Zhang, M.; Xu, J.-G.; Zhang, N.-N.; Lu, J.; Xin, X.-H.; Zheng, F.-K.; Guo, G.-C. A highly stable and tightly packed 3D energetic coordination polymer assembled from nitrogen-rich tetrazole derivatives. *New J. Chem.* **2018**, *42*, 13927−13932.
(35) Du, Y.; Su, H.; Fei, T.; Hu, B.; Zhang, J.; Li, S.; Pang, S.; Nie, F. Structure-Property Relationship in Energetic Cationic Metal-Organic Frameworks: New Insight for Design of Advanced Energetic Materials. *Cryst. Growth Des.* **2018**, *18*, 5896−5903.
(36) Wang, S.; Wang, Q.; Feng, X.; Wang, B.; Yang, L. Explosives in the Cage: Metal-Organic Frameworks for High-Energy Materials Sensing and Desensitization. *Adv. Mater.* **2017**, *29*, No. 1701898.
(37) Demko, Z. P.; Sharpless, K. B. Preparation of 5-substituted 1 H-tetrazoles from nitriles in water. *J. Org. Chem.* **2001**, *66*, 7945−7950.
(38) Liu, X.; Yang, Q.; Su, Z.; Chen, S.; Xie, G.; Wei, Q.; Gao, S. 3D high-energy-density and low sensitivity materials: synthesis, structure and physicochemical properties of an azide-Cu(ii) complex with 3,5-dinitrobenzoic acid. *RSC Adv.* **2014**, *4*, 16087−16093.
(39) Qu, X.; Yang, Q.; Han, J.; Wei, Q.; Xie, G.; Chen, S.; Gao, S. High performance 5-aminotetrazole-based energetic MOF and its catalytic effect on decomposition of RDX. *RSC Adv.* **2016**, *6*, 46212−46217.
(40) Rouse, P. E., Jr. Enthalpies of formation and calculated detonation properties of some thermally stable explosives. *J. Chem. Eng. Data* **1976**, *21*, 16−20.
(41) Krien, G.; Licht, H.; Zierath, J. Thermochemische untersuchungen an nitraminen. *Thermochim. Acta* **1973**, *6*, 465−472.
(42) Cox, J.; Wagman, D. D.; Medvedev, V. A. *CODATA Key Values for Thermodynamics*; Hemisphere Publishing Corporation, 1989.
(43) Kamlet, M. J.; Jacobs, S. Chemistry of detonations. I. A simple method for calculating detonation properties of C-H-N-O explosives. *J. Chem. Phys.* **1968**, *48*, 23−35.
(44) Wang, Y.; Zhang, J.; Su, H.; Li, S.; Zhang, S.; Pang, S. A simple method for the prediction of the detonation performances of metal-containing explosives. *J. Phys. Chem. A* **2014**, *118*, 4575−4581.
(45) Kissinger, H. E. Reaction kinetics in differential thermal analysis. *Anal. Chem.* **1957**, *29*, 1702−1706.
(46) Ozawa, T. A new method of analyzing thermogravimetric data. *Bull. Chem. Soc. Jpn.* **1965**, *38*, 1881−1886.
(47) Doyle, C. D. Kinetic analysis of thermogravimetric data. *J. Appl. Polym. Sci.* **1961**, *5*, 285−292.
(48) Harris, J. Autoignition temperatures of military high explosives by differential thermal analysis. *Thermochim. Acta* **1976**, *14*, 183−199.
(49) Bruker. *APEX2, SAINT and SADABS*; Bruker AXS Inc.: Madison, Wisconsin, 2012.
(50) Sheldrick, G. M. A short history of SHELX. *Acta Crystallogr., Sect. A: Found. Crystallogr.* **2008**, *64*, 112−122.
(51) Dubbeldam, D.; Calero, S.; Vlugt, T. J. iRASPA: GPU-accelerated visualization software for materials scientists. *Mol. Simul.* **2018**, *44*, 653−676.

DOI: 10.1021/acsomega.9b01127
ACS Omega XXXX, XXX, XXX−XXX